J. exp. Biol. 152, 189–209 (1990)
Printed in Great Britain © The Company of Biologists Limited 1990

PLATEAU-GENERATING NERVE CELLS IN *HELIX*: MORPHOLOGICAL AND ELECTROPHYSIOLOGICAL CHARACTERISTICS

BY T. PIN, M. CREST, E. EHILE, G. JACQUET AND M. GOLA*

Laboratoire de Neurobiologie, CNRS, 31 Chemin Joseph-Aiguier, 13402 Marseille, Cedex, France

Accepted 24 May 1990

Summary

We describe the anatomical and electrophysiological characteristics of a group of *Helix* nerve cells, styled P cells, that generate long-lasting depolarizations in response to repeated stimulations at low frequencies. Four neurones were identified in the perioesophageal ganglia of the snail *Helix pomatia*. Their structure was determined by intracellular injection of Lucifer Yellow, cobalt–lysine or horseradish peroxidase. The soma was found to contain neurosecretory granules. These cells innervated the whole foot muscle and the mantle, but were not involved in muscle movement or locomotion. They may participate in mucus secretion. Upon depolarization they fired Ca^{2+}-dependent spikes; at a critical firing rate (5–6 Hz), the spikes were converted into depolarized plateaus (+10 to +20 mV) lasting for several seconds. The plateau was Ca^{2+}-dependent and persisted in Na^+-free saline. It was sustained by a slowly inactivating Ca^{2+} current that produced a large intracellular Ca^{2+} accumulation (monitored with the Ca^{2+}-sensitive dye Arsenazo III). The plateau was restricted to the soma and the proximal axon and may act as a driver potential inducing axon firing and prolonging the release of neurosecretory materials.

Introduction

The signalling properties of nerve cells largely depend on the presence of Ca^{2+} channels. Unlike cells that generate stereotyped Na^+-dependent action potentials, nerve cells endowed with Ca^{2+} channels display a large variety of electrical signals. Ca^{2+}-dependent action potentials may last from a few milliseconds to several seconds. This variety is largely attributable to the properties of Ca^{2+} currents, which are characterized by a slow, persistent activation, and to the feedback control exerted by intracellular calcium on various channels. Depolarizations induced by persistent Ca^{2+} entries are generally counteracted by repolarizing currents subsequently triggered either by cell depolarization or by intracellular

* To whom reprint requests should be addressed.

Key words: mollusc, *Helix pomatia*, neurones, Ca^{2+} spikes, paroxysmal depolarization.

calcium accumulation. In various experimental and pathological situations, feedback repolarizing currents may be depressed, which may result in long-lasting depolarizations closely resembling the paroxysmal discharges observed in cortical epileptic foci.

Long-lasting Ca^{2+}-dependent spikes have been described in various molluscan nerve cells subjected to repeated stimulation (see Edstrom and Lukowiak, 1985). The spike enlargement has generally been ascribed to a progressive blockade of the repolarizing currents (Eckert and Lux, 1977; Aldrich *et al.* 1979). The enlargement is nevertheless limited in duration, since Ca^{2+} channels are themselves blocked by repetitive pulsing.

In the central nervous system of the land snail *Helix pomatia* we identified a group of four neurones that generated purely Ca^{2+}-dependent spikes. Isolated spikes had relatively short durations (approx. 6 ms). In response to repetitive pulsing at low rates (<6 Hz), the spike progressively enlarged, as previously reported in the case of several molluscan nerve cells, but it was suddenly converted into a prolonged depolarization which could last for tens of seconds. To our knowledge, no such behaviour has ever been reported in nerve cells maintained in almost physiological conditions.

The aims of the present and following paper were (1) to give an exhaustive description of the electrophysiological and morphological properties of the plateau-generating cells and (2) to elucidate the ionic mechanisms which led to the change from firing to a depolarized plateau.

Materials and methods

Experiments were performed on nerve cells of the perioesophageal ganglion of the snail *Helix pomatia*. Four plateau-generating cells (P cells) were identified in the right parietal and visceral ganglia (see Fig. 1). Most of the experiments were carried out on the P1 cell located in the caudal part of the visceral ganglion. A plateau-generating cell located in the same region was also identified in the species *Helix aspersa*; this cell might correspond to the E4 cell described by Kerkut *et al.* (1975). Some of the electrophysiological properties of the P1 cell have been reported by Labos (1969). A comparative study was performed with three other nerve cell groups: two large neurones located in the rostral parietal ganglia (cells 3 and 20, Walker *et al.* 1970), two bursting cells (Pin and Gola, 1984) and the U cell cluster in the right parietal ganglion (Lux and Hofmeier, 1982). These cells will be denoted A, Br and U, respectively. They were selected on the basis of the large Ca^{2+} current that was induced by soma depolarization under voltage-clamp conditions. Ganglia were excised and the pallial, pleural and visceral ganglia were separated from the inner layer of pedal ganglia by undercutting the parieto-pedal connectives. The connective tissue was softened by a 2–5 min treatment with Protease (Sigma type XIV) and removed with sharpened forceps. No attempt was made to isolate the nerve cell bodies from the axon trunk.

Cells were impaled with a voltage-recording electrode (2–4 MΩ) and with a

current-injecting electrode (1.5–2 MΩ), both filled with 3 mol l^{-1} KCl. They were studied under conventional current-clamp or voltage-clamp conditions. The reference electrode was a large pipette filled with 3 mol l^{-1} KCl–agar, positioned near the ganglia in order to minimize the series resistance (evaluated to be 3.5–8 kΩ), which was not compensated for. Since the peak Ca^{2+} current in these cells was less than 300 nA, the voltage error introduced by the series resistance was less than 3 mV. In the following paper, which deals with large outward currents (up to 2 μA), the series resistance was liable significantly to distort the actual potential applied to the membrane.

Intracellular injections were performed from a third intracellular microelectrode filled with either 1 mol l^{-1} tetraethylammonium chloride (TEACl) or 0.7 mol l^{-1} EGTA (K^+ salt) (tip resistance: 20–25 MΩ). Ionophoretic injections (current ranging from 25 to 100 nA, 0.5 s pulses applied at 1 Hz) were performed while the cell was voltage-clamped at −50 mV holding potential, so that no change in the net membrane current occurred during injection.

The cell morphology (cell body, axon branches and dendritic processes) was determined by injecting Lucifer Yellow from microelectrodes filled with a 5 % aqueous solution of the dye (tip resistance: 30–60 MΩ). Injections with 20–40 nA negative current pulses lasted 1.5–3 h. To detect remote axon and dendritic processes, injected cells were occasionally maintained at room temperature for 2–5 h. Ganglia were then fixed for 8 h in 4 % formaldehyde, dehydrated and cleared in methylsalicylate. They were observed in a Leitz fluorescence microscope and photographed with Kodak Ektachrome 400ASA film.

Additional morphological data were obtained from cobalt–lysine- injected cells. In comparison to Lucifer Yellow, cobalt–lysine gave more accurate details of the dendritic-like structures, spine processes and boutons, although it proved to be less efficient in detecting remote processes. The cobalt solution was prepared using the method described by Altrup and Peters (1982). Injections with cobalt–lysine-filled microelectrodes (tip resistance: 20–40 MΩ) lasted 1.5–3 h. Cobalt was precipitated with 0.2 % ammonium sulphide added to the saline. Ganglia were then fixed for 8 h in 10 % formaldehyde. They were silver-intensified using the Altrup–Peters method, except for the pre-treatment, where the Pronase intended to permeabilize the membrane was replaced by 1 % Triton X100 added to the Timm B solution (Croll, 1986). The ganglia were then dehydrated and cleared with methylsalicylate for whole-mount observations.

The ultrastructure of P cells was determined from horseradish-peroxidase (HRP)-labelled cells. HRP (type VI, Sigma) was ionophoretically injected from a microelectrode filled with 4 % HRP. Injections with 5–10 nA positive current pulses lasted 4 h. Ganglia were then fixed in 4 % glutaraldehyde, washed in 0.05 mol l^{-1} cacodylate buffer, and pre-incubated for 1 h in 0.1 % 3.3′-diaminobenzidine (DAB, Sigma) in 0.05 mol l^{-1} Tris buffer (pH 7.6). The HRP–DAB reaction was induced by adding 0.003 % H_2O_2 for 15–40 min. When the cell body had taken on a dark-brown colour, the reaction was stopped by several washings in Tris saline. Ganglia were post-fixed in 2 % osmium tetroxide (2 h) and convention-

ally processed for electron microscopy. Ultra-thin sections were stained with lead citrate and uranyl acetate and examined with a Zeiss 109 electron microscope.

The physiological saline had the following composition (in $mmol\,l^{-1}$): NaCl, 75; KCl, 5; $CaCl_2$ and $MgCl_2$, 8; Tris (pH 7.5), 5. In Na^+-free salines, Na^+ was replaced by 90 $mmol\,l^{-1}$ Tris. The Ca^{2+} content varied from 0 to 16 $mmol\,l^{-1}$ (osmolarity maintained at 200–210 $mosmol\,l^{-1}$ by adjusting the Tris concentration). Ca^{2+} currents were studied in TEA^+- and EGTA-injected cells bathed in salines in which Na^+ was replaced by 60 $mmol\,l^{-1}$ TEA^+ and 10 $mmol\,l^{-1}$ 4-aminopyridine (4-AP).

Changes in intracellular Ca^{2+} concentration were measured using the Ca^{2+}-sensitive dye Arsenazo III, intracellularly injected with a microelectrode filled with a 10–15 $mmol\,l^{-1}$ aqueous solution of the K^+ salt of the dye. Injections with 10–40 nA negative current pulses (10–15 min) were monitored by measuring the increase in the cell absorbance at 570 nm. Final dye concentration was evaluated at 0.3–0.5 $mmol\,l^{-1}$. Absorbance changes were measured differentially at three different wavelengths (570, 650 and 690 nm) with a light-pulsed spectrophotometer constructed by ourselves as described by Gorman and Thomas (1978). Light from a quartz iodide source passed through a rapidly spinning rotor (2–3000 revs min^{-1}) which contained three narrow-band interference filters. The light passing through the cell was collected by an 80 μm diameter optic fibre located close to the cell and led to a photodiode. Any absorbance changes occurring during cell activity were measured with the 650–690 nm filters.

Results

Morphology of the plateau-generating cells

Fifteen P cells were stained with Lucifer Yellow: 10 P1, two P2, two P3 and one P4. In three experiments, two P cells were simultaneously dye-filled. Although the cells were located in different parts of the nervous system, they had similar axonal and dendritic distributions. Fig. 1 shows photomicrographs and drawings of a dye-filled P1 cell. Drawings were obtained from whole-mount photomicrographs taken from the ventral and dorsal surfaces of the ganglia complex cleared from the pedal ganglia layer. The locations of the cell body and of the main axon branches of the P1 cell are shown in Fig. 1C. A plateau-generating cell with a similar morphology was also identified in the caudal part of the visceral ganglion of the species *Helix aspersa*.

The P1 monopolar nerve cell body (120–160 μm in diameter) sent a large axon (40–50 μm) into the visceral neuropile, where it split into two branches (20–30 μm in diameter) running towards the right and left pleural ganglia. Thin branches emerged from the two main axons and ran towards the five nerves that emerged from the ganglia. A similar morphology was observed in dye-filled P2, P3 and P4 cells (Fig. 2). The 15 injected cells displayed slight variations in the number of efferent axon branches: 1–3 in the right and left pallial nerves, and 0–1 in the visceral, anal and pallio-cutaneous nerves. The two main axon branches ended

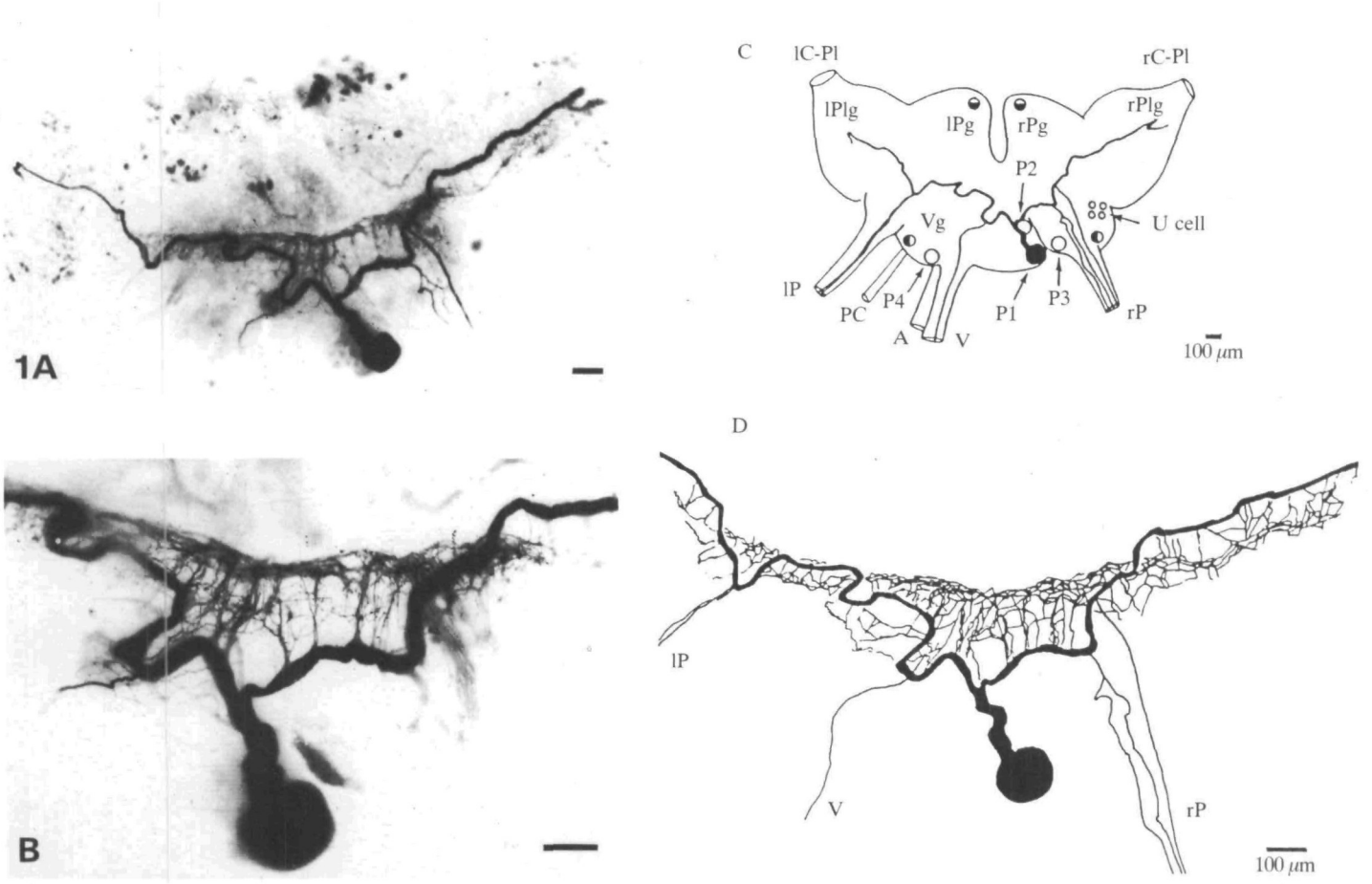

Fig. 1. Morphology of the plateau-generating P1 cell. Whole-mount photomicrographs (A and B) and drawings (C, D) of a Lucifer-Yellow-filled P1 cell. (A, C) Dorsal views of the cell morphology within the ganglion complex; (B, D) details of the dendritic-like processes. Scale bars, 100 μm. In this and subsequent figures, letters have been assigned as follows: ganglia: lPlg and rPlg, left and right pleural ganglia; lPg and rPg, left and right parietal ganglia; Vg, visceral ganglion; nerves: lP and rP, left and right pallial nerves; PC, A and V, pallial-cutaneous, anal and visceral nerves; connectives: lC-Pl and rC-Pl: left and right cerebro-pleural connectives. P1–P4, P cells 1–4. ◐ Bursting cell; ◒ A cell.

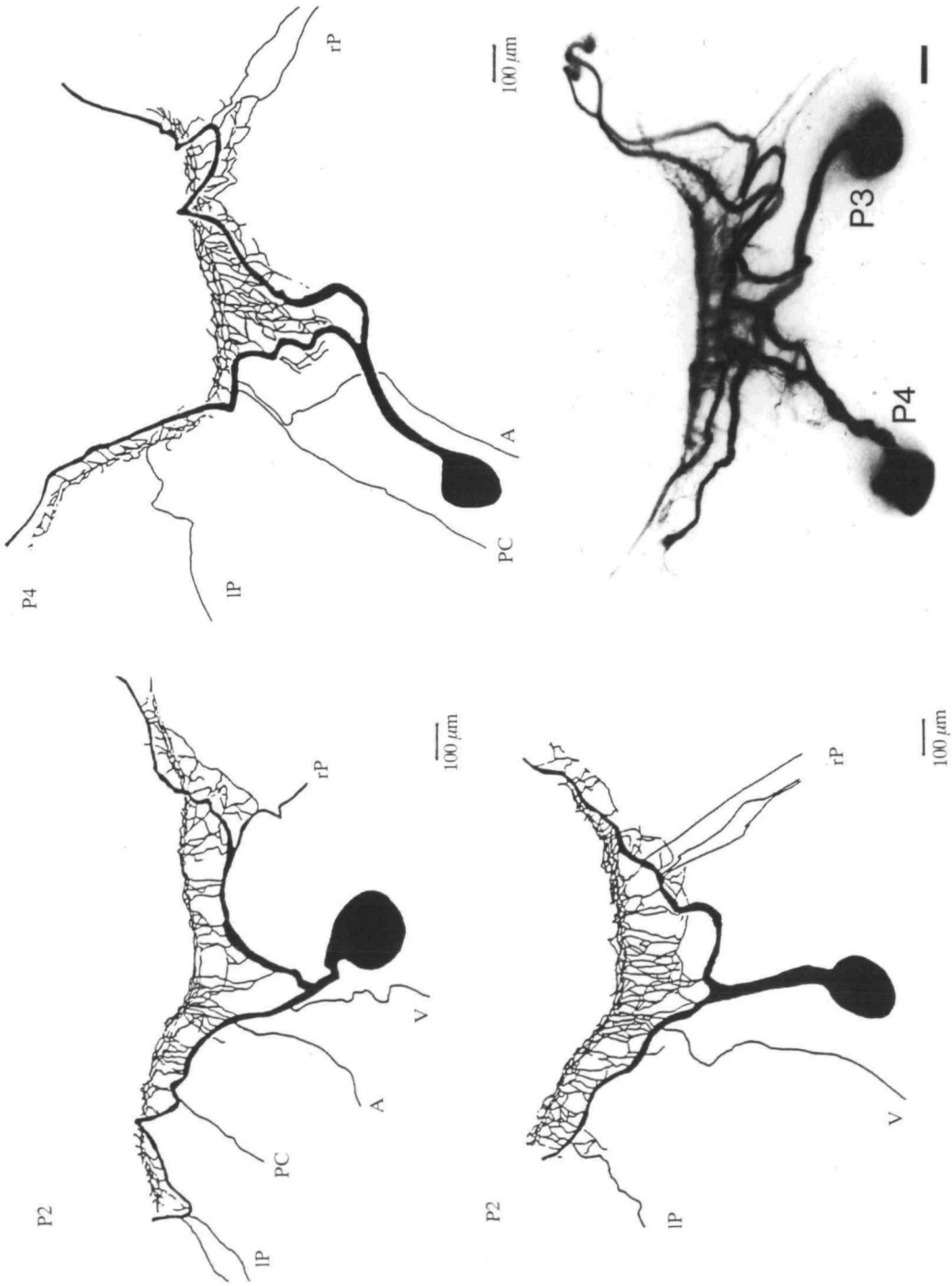

Fig. 2. Morphology of the P2–P4 plateau-generating cells. Drawings and photomicrographs are dorsal views of Lucifer-Yellow-injected cells. The double labelling of the P3 and P4 cells was obtained by simultaneous dye-filling. See Fig. 1 for the location of the

within the neuropile of the left and right pleural ganglia. They occasionally sent very thin processes into the cerebro-pleural connective. An almost identical morphology has been described in a Procion-Yellow-injected cell in *Helix aspersa*: cell 4 described by Kerkut *et al.* (1970) or cell E10 by Kerkut *et al.* (1975). The location of this cell, close to the anal nerve, makes it homologous to the P4 cell in *Helix pomatia*.

The idea that the plateau-generating cells may perform similar physiological functions was based on the finding that their electrophysiological and morphological characteristics were identical. For instance, although the P3 and P4 cells were located in two different ganglia, they had an almost symmetrical appearance and identically distributed axon and dendritic processes (Fig. 2).

The most striking feature of the P cells concerned the structure of the dendritic-like processes. These processes were located within the neuropile of the ganglia, all along the two main axon branches. They emerged from these axons and ran rostrally to form a net spreading over the whole ganglia. The structure of the processes was more clearly resolved in cobalt–lysine-injected cells (Fig. 3). No major difference from the Lucifer Yellow method was noted as regards the general morphology of the cells. Nevertheless, the cobalt–lysine method revealed that the thin processes extending within the visceral neuropile displayed an extensive branching with a spiny appearance (Fig. 3B), suggesting that they have a postsynaptic function. This interpretation was not corroborated by the electrophysiological data, since there was characteristically no background synaptic noise in these cells; however, the remote location of the synaptic inputs from the recording site in the soma might partly account for this discrepancy.

Because of the small diameter of the axon branches within the efferent nerves, extracellular platinum electrodes (insulated with a drop of liquid paraffin), placed on the nerves freed from the connective sheath, generally failed to detect a signal when the soma was fired. With a signal averager, a somato-fugal axon signal locked to the soma spike was recorded in all the efferent nerves. Stimulation of these nerves failed, however, to induce antidromic responses, as reported in the case of the E4 cell in *Helix aspersa* (Kerkut *et al.* 1975); this was probably the result of a spike blockade at the branching points where the thin axons emerged from the two main branches. Depolarizing the soma membrane did not result in antidromic responses. On increasing the nerve stimulation, antidromic responses were occasionally observed. Their antidromic nature was checked by applying a simultaneous stimulus to the soma, which induced spike collision within the neuropile. The antidromic responses did not, however, show a constant latency, and they were superimposed on long-lasting, 2–5 mV amplitude synaptic potentials. They were probably produced by synaptic potentials induced in the remote dendritic net by presynaptic fibres running in the stimulated nerves. From the initiating area located within the neuropile, spikes are likely to have propagated in both directions, distally and towards the soma. These data establish that P cells may have a motor function; they may receive information at the level of the neuropile processes and send efferent spikes into the various axon branches. This

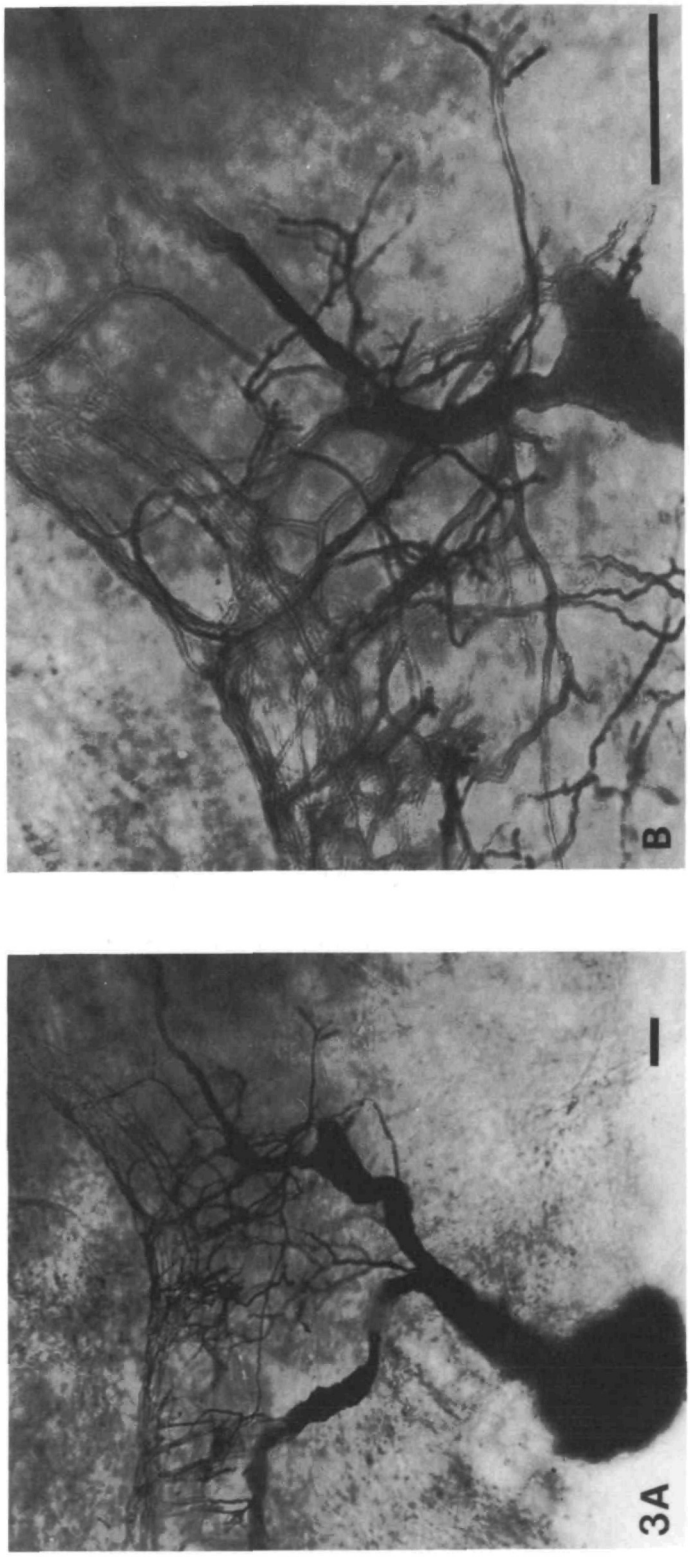

Fig. 3. (A,B) Photomicrographs of a cobalt–lysine-injected P1 cell. Ventral views of the dendritic-like processes within the neuropile. Note the numerous branches and spiny appearance of the processes in the enlarged view. Scale-bars, 50 μm.

hypothesis was strengthened by the finding that stimulation of the right or left cerebro-pleural connectives produced long-lasting discharges in P cells. The discharges were produced by both fast and slow depolarizing synaptic potentials from which spikes antidromically invaded the cell body. A brief connective stimulation produced discharges with a duration of several seconds, during which the spikes showed the typical enlargement observed under direct soma stimulation (see below).

To improve the detection of the fine processes within the neuropile, the whole-mount photographs illustrated in Figs 1 and 2 were taken from ganglia that were separated from the pedal ganglia. Additional electrophysiological and dye-filling experiments were performed with the intact perioesophageal ring. Under these conditions, however, the distribution of axonic and dendritic processes within the neuropiles could not be resolved. These experiments showed that the two main axon branches which seemed to end within the pleural ganglia actually entered the left and right parieto-pedal connectives and ran towards the pedal ganglia. Within the pedal neuropiles, each axon sent branches into each pedal nerve. Using a signal averager, it was possible to record efferent axon spikes in these nerves in response to soma stimulation (Fig. 4A).

The schematic axon distribution of a P cell is shown in Fig. 4B. Axon branches running in the pedal nerves innervated the foot muscle. The branches within the right and left pallial nerves distributed to the anterior mantle. The infrequent axon branches observed in the visceral, anal and pallio-cutaneous nerves had an unknown distribution. Additional experiments were performed in ganglia maintained in the animal. Access to the P cells was obtained by cutting the dorsal muscle longitudinally. These *in toto* experiments, with intact nerves and connectives, failed to reveal any muscle movements in response to a firing P cell. This axon distribution is reminiscent of that of the *Aplysia* R2 and LPl1 neurones, which innervate the foot muscle where they produce mucus secretion (Rayport *et al.* 1983).

P cells as well as bursting cells were whitish under direct illumination. This appearance suggested that P cells might be neurosecretory. The ultrastructure of P cells was examined after intracellular injection with HRP. Stained cells were identified in semi-thin sections and further processed for electron microscopy. The cytoplasm of the soma body and that of the axon hillock contained medium-sized secretory granules (90–210 nm in diameter; mean 140 nm) (Fig. 5A). The granules were membrane-bound and had an electron-dense content (Fig. 5C). The presence of these granules suggested that P cells may have a neurosecretory function. They were shown to have a high level of synthetic activity by the presence of numerous well-developed Golgi complexes surrounded by immature granules as well as dilated cisternae of rough endoplasmic reticulum filled with an electron-lucent material (Fig. 5B).

Electrophysiological characteristics

Unlike many neurosecretory cells from invertebrates, P cells were always silent,

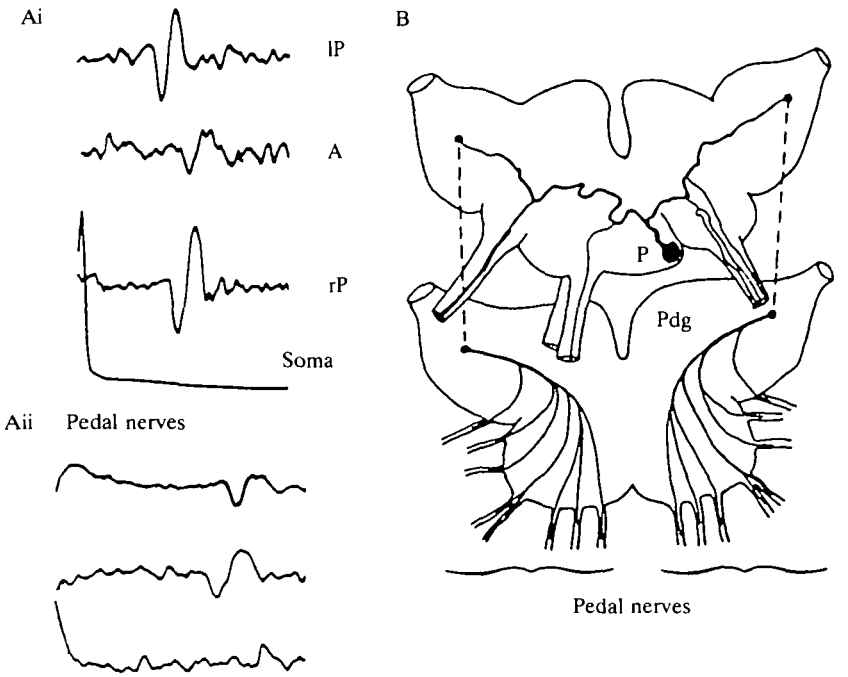

Fig. 4. Peripheral axon projection of P cells. (A) Recordings of axon spikes in peripheral nerves in response to soma stimulation of a P cell. Axon spikes were recorded with monopolar platinum electrodes located on the efferent nerves from the perioesophageal ganglion complex (Ai) and on pedal nerves (Aii). Signals extracted from background nerve activity by a digitized averager were locked to the soma spike (30–60 successive sweeps). (B) Peripheral axon projections of P cells: reconstruction based on Lucifer-Yellow-injected cells and electrophysiological data. The pedal ganglia (Pdg) were actually closely apposed to the parieto-visceral ganglion complex; the dotted lines indicate the axon trajectory within the parieto-pedal connectives.

with a resting potential ranging from −55 to −60 mV (mean±S.D.: 58±5 mV, N=28). Similar values and lack of spontaneous activity were observed in ganglia still connected to the pedal and cerebral ganglia (*in toto* experiments). Simultaneous recordings from two P cells performed within the same ganglion failed to reveal any electrical coupling during either spiking periods or depolarized plateaus.

Stimulation of the soma with a long-lasting depolarizing current elicited overshooting spikes. The first spike in the discharge occurred after a latent period known as the 'break response' which has been attributed to the transient activation of the fast A current (see review by Rogawski, 1985). To facilitate spike production by short current pulses, the soma was depolarized at −50 mV, which inactivated the A current. The spike had a large amplitude (80–105 mV peak amplitude) and its duration measured at half-amplitude was 6.5 ms. The overshoot was +39±5 mV (N=18) and the depolarizing and repolarizing rates ranged between 10 and 14 $V s^{-1}$.

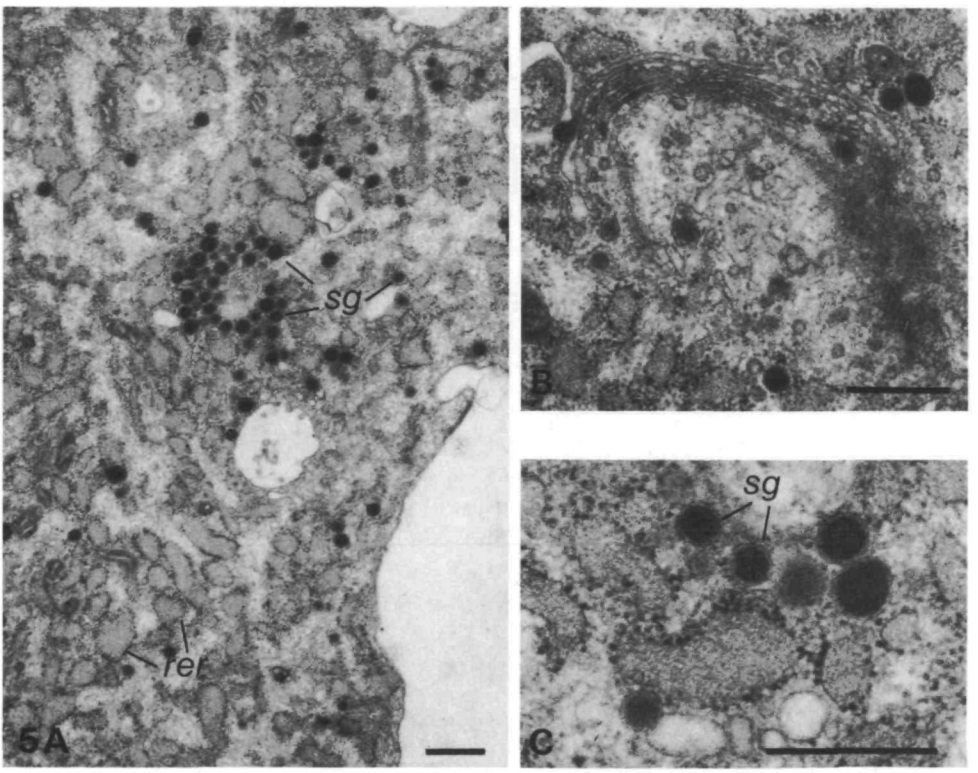

Fig. 5. Ultrastructure of plateau-generating cells. P1 cell intracellularly injected with horseradish peroxidase. (A) Low-magnification view of the cell body cytoplasm filled with numerous electron-dense secretory granules *(sg)* and cisternae of rough endoplasmic reticulum *(rer)* with membrane-bound ribosomes. (B, C) Enlarged view of a golgi complex (B) surrounded by immature and mature secretory granules. The secretory granules (C) had a homogeneous electron-dense content and a mean diameter of 140 nm. Scale bars, 0.5 μm.

The spike parameters were very sensitive to the firing rate. Fig. 6 illustrates the change in the spike shape that occurred under repeated stimulations at relatively low rates (1–5 Hz). The spike enlarged consistently during firing, particularly at frequencies above 4 Hz. Between 5 and 6 Hz, the spike duration increased dramatically and when the spike duration reached 40–50 ms, a long-lasting depolarized plateau developed (Fig. 6Bii). The transition from the firing mode to the depolarized plateau occurred sharply and could be induced either by repeated pulsing or by sustained depolarization with a long-lasting outward current (Fig. 6C). Once the plateau had been triggered, the stimulating outward current was no longer necessary for it to be sustained.

The plateau was at a positive level (between +10 and +20 mV). The plateau duration varied considerably from one cell to another and depended on the duration of the rest period between two successive plateaus. Its mean duration was

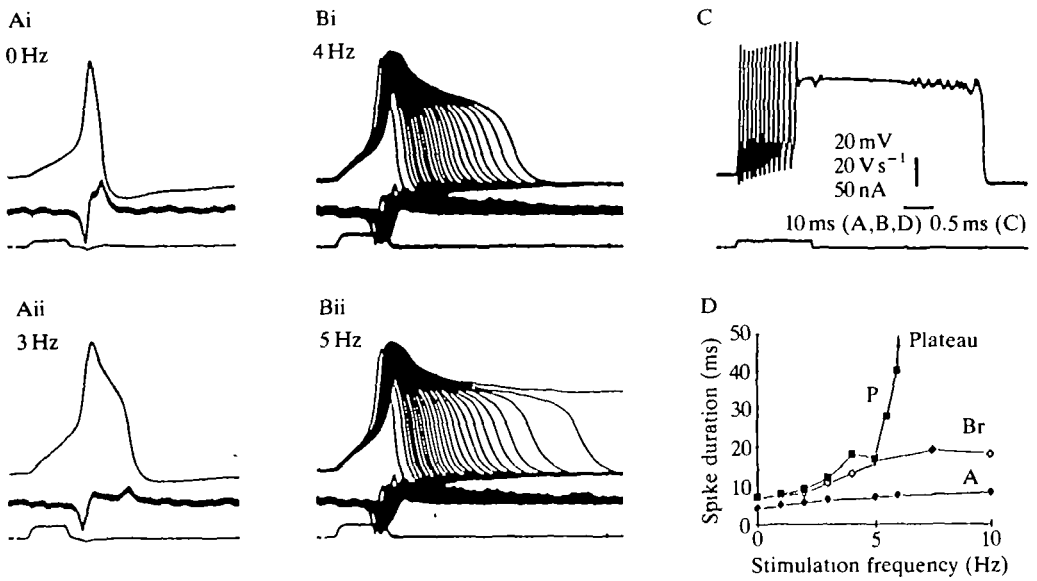

Fig. 6. Frequency-dependent spike broadening and long-lasting plateaus in stimulated P cells. Each recording in series A and B shows (from top to bottom) the membrane potential, its first derivative (inverted) and the stimulating current. (A) Spikes recorded in a P cell fired with short current pulses applied at different frequencies. Recordings were made when the steady-state spike pattern was achieved. (B) Superimposed spikes during repetitive stimulations at 4 Hz (Bi) and 5 Hz (Bii). In Bii, the repolarizing phase was progressively delayed and finally aborted. (C) Long-lasting (3.2 s) plateau in response to a step depolarization. Note that the plateau persisted after the current pulse. Vertical bar: 20 mV, 20 V s^{-1} and 50 nA. Horizontal bar: 10 ms, except in C, 0.5 s. (D) Spike duration (measured at half-amplitude) *versus* firing frequency; data pooled from 14 P cells (■), five bursting cells (◇) and 11 A cells (◆). The vertical arrow indicates the mean firing frequency required for the spike–plateau transition to occur.

between 2 and 3 s, but it could last for 20–30 s after a 10 min rest period at −60 mV. It is notable that the spike enlargement preceding the plateau occurred without any significant change in the spike depolarizing rate (indicated by the first derivative of the voltage in Fig. 6). By contrast, the spike repolarization gradually slowed down, indicating that the enlargement was probably due to a decrease in the repolarizing potassium currents.

The plateau potential must result from a delicate balance of ionic currents in which Ca^{2+} and K^+ are involved (see below and following paper). This balance was easily disturbed by applied current pulses. When P cells were simultaneously impaled with several low-resistance intracellular electrodes, the plateaus were of short duration, presumably because of the increased leakage current resulting from injury. This leakage current did not prevent the voltage shift to the plateau, but it consistently reduced the plateau duration (see Fig. 9).

The same experiments were performed in the three other nerve cell groups. On

the basis of voltage-clamp experiments, A cells were found to be closely related to P cells (see Crest *et al.* 1990). Upon repeated stimulation, the A cell spike displayed a slight enlargement. The enlargement, however, had a limited amplitude; the spike duration did not exceed 10 ms even at a firing frequency of 10 Hz. The difference between A and P cells is illustrated in the diagram in Fig. 6D, in which the spike duration is shown as a function of the firing frequency. Bursting cells showed an intermediate behaviour; as in P cells, the spike had a typical shoulder on the repolarizing phase. Regular firing produced a spike enlargement which reached a peak value (20–25 ms in duration) at 4–5 Hz. Higher frequencies reduced both spike amplitude and duration. In the purely Ca^{2+}-dependent U cell spike (Lux and Hofmeier, 1982), no, or only moderate, spike lengthening was observed. The relatively long-lasting spike (15–20 ms in duration) observed in resting U cells tended to be reduced and shortened by regular pulsing at 1–3 Hz (Gola *et al.* 1986).

Ionic requirements of the spike–plateau pattern

Long-lasting spikes are generally thought to reflect a calcium contribution to the inward current. When a P cell was bathed in a low-calcium (1 mmol l^{-1}) saline, spikes were considerably depressed or even blocked. Plateaus could no longer be induced by long-lasting currents (Fig. 7). Ca^{2+}-free salines, some containing a Ca^{2+} channel blocker (2 mmol l^{-1} Cd^{2+}, 8 mmol l^{-1} Co^{2+} or 1 mmol l^{-1} La^{3+}), fully suppressed spikes and plateaus.

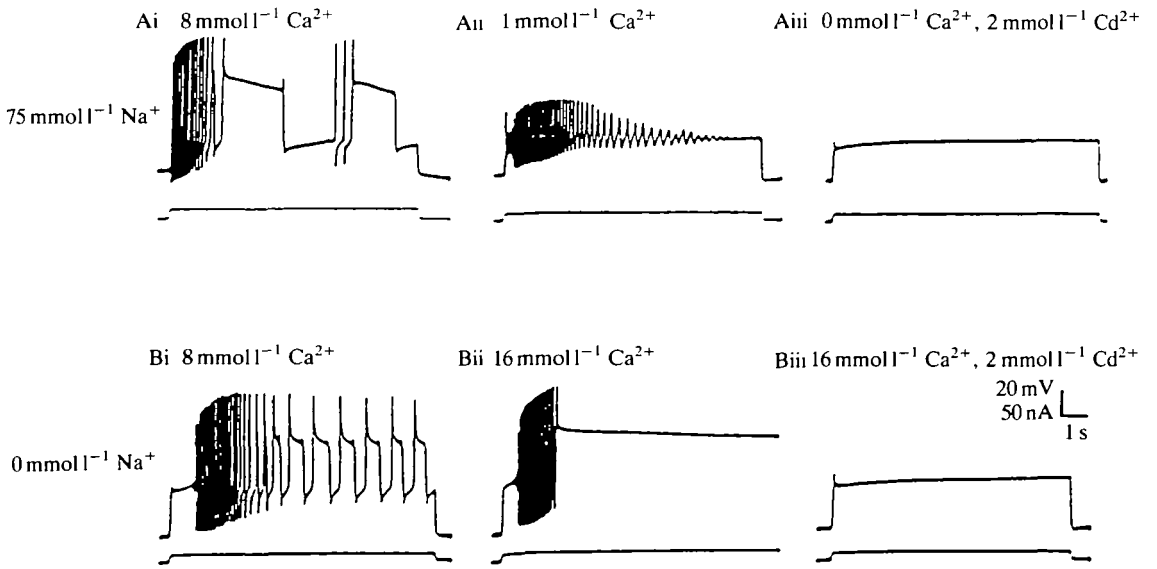

Fig. 7. Ionic dependency of the plateau. Series A and B were performed in the presence of 75 mmol l^{-1} Na^+ (A) and in Na^+-free saline (B). Spikes and plateaus were reduced or blocked in low-Ca^{2+} saline (Aii) and in the presence of Ca^{2+} channel blockers (2 mmol l^{-1} Cd^{2+} in Aiii and Biii). The plateau persisted in the absence of sodium and was enhanced in high-Ca^{2+} saline (Bii).

Conversely, the spike–plateau pattern persisted in Na^+-free salines (Na^+ replaced by Tris), although the plateaus were generally shortened (Fig. 7B). Plateaus lasting for several seconds were produced when the Ca^{2+} content of the Na^+-free saline was increased from 8 to 16 mmol l^{-1} (Fig. 7Bii); these plateaus were blocked by adding a Ca^{2+} channel blocker to the Na^+-free saline. Replacing calcium in the Na^+-free saline by an equimolar amount of strontium or barium favoured the occurrence of long-lasting plateaus.

From these data it was clear that the depolarized plateaus were sustained by a persistent Ca^{2+} current, although the possibility of a sodium contribution to the spike could not be excluded. These hypotheses were checked by changing the Ca^{2+} content (from 0.5 to 32 mmol l^{-1}) of salines, some containing sodium. Changes in the Ca^{2+} concentration of the Na^+-free saline produced a change in the spike overshoot which obeyed the Nernst equation for a Ca^{2+}-selective process: a 29 mV change in spike overshoot with a 10-fold change in $[Ca^{2+}]$ (Fig. 8A). The same relationship was observed in the presence of sodium ions (75 mmol l^{-1}) (Fig. 8B,C). Spikes persisted when calcium was replaced by an equimolar amount of strontium or barium in the Na^+-free saline. Their overshoot still showed a 29 mV change per 10-fold change in either ion concentration. Magnesium was found to be less effective.

These data indicate that sodium ions did not play a significant role in spikes and plateaus. The P cells therefore produced almost purely Ca^{2+}-dependent spikes. Spikes depending solely on calcium ions have been observed in a few nerve cells: in *Helix* U cells (Lux and Hofmeier, 1982) and in the LGC cells in the leech (Johansen *et al.* 1987). Because of the slow activation rate of Ca^{2+} currents in comparison with Na^+ currents, the purely Ca^{2+}-dependent spikes had a slow onset: the maximal depolarizing rates in P cells and in U cells were as low as 14 V s^{-1}. The corresponding figures for Na^+-dependent spikes in *Helix* nerve cells ranged from 40 to 60 V s^{-1}.

A persistent calcium current sustains the depolarized plateau

Calcium entry during the depolarized plateau produced a consistent intracellular $[Ca^{2+}]_i$ increase. Relative $[Ca^{2+}]_i$ changes during the spike–plateau pattern were monitored by measuring changes in the absorbance of the intracellularly injected Ca^{2+}-sensitive dye Arsenazo III. In Na^+-free saline, a spike burst induced a sharp increase in $[Ca^{2+}]_i$. After the burst, the optical signal slowly returned to its base level with time constants of 8–15 s (Fig. 9A). Under favourable conditions, the increase in the optical signal was resolved into discrete step changes corresponding to successive spikes. At the burst–plateau transition, a very large increase was observed in the optical signal, which developed along the whole plateau (Fig. 9B).

Ca^{2+} currents were detected in P cells from which outward and leakage currents had been eliminated. The sodium content of the perfusing saline was replaced by 60 mmol l^{-1} TEA^+ and 10 mmol l^{-1} 4-AP. Under these conditions, the sodium current, the fast transient A current and the Ca^{2+}-activated K^+ current were

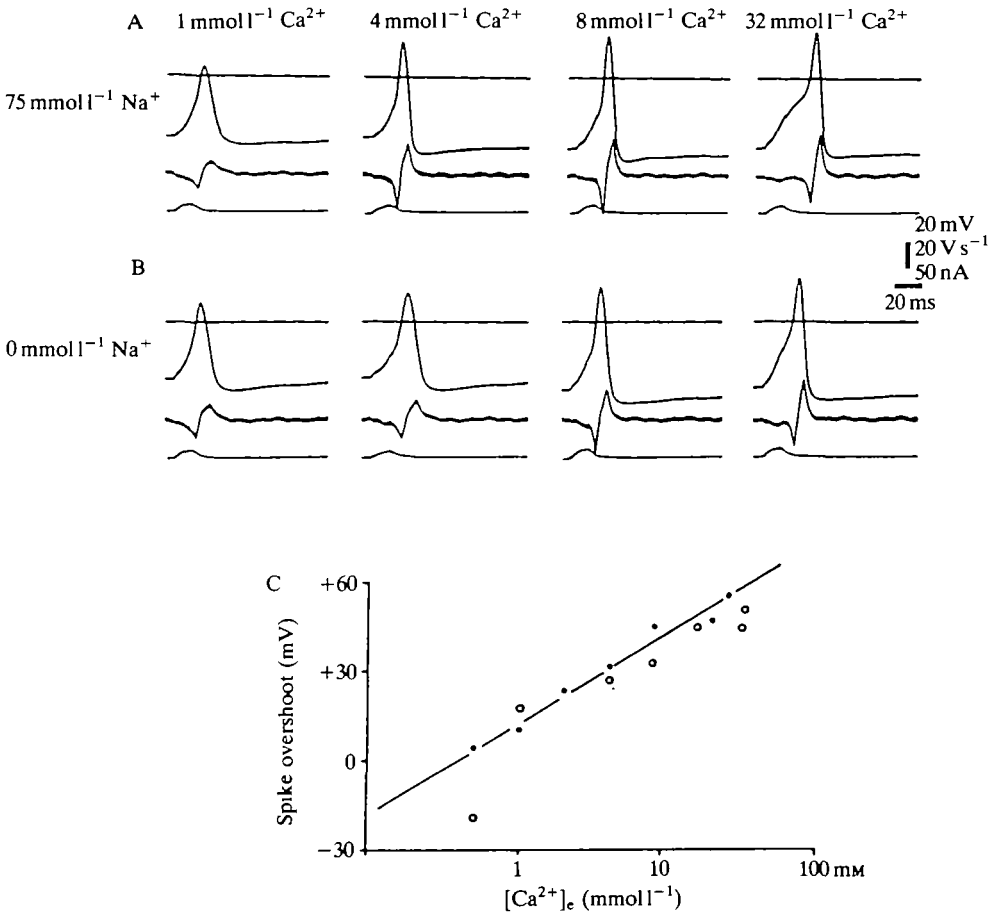

Fig. 8. Ionic dependency of P cell spikes. The Ca^{2+} content of the saline was changed from 1 to 32 mmol l^{-1} in the presence of normal Na^+ concentration (series A) and in Na^+-free saline (series B). (C) Spike overshoot *versus* Ca^{2+} concentration (on a logarithmic scale). The straight line was drawn through experimental points with a slope of 29 mV per 10-fold change in $[Ca^{2+}]$. ● 0 mmol l^{-1} Na^+; ○ 75 mmol l^{-1} Na^+.

completely suppressed. Part of the voltage-gated K^+ current, however, still persisted. It was fully suppressed after an intracellular injection of TEA^+ (see Crest *et al.* 1990). In some experiments, P cells were successively injected with TEA^+ and EGTA. The leakage current was routinely eliminated using a 50 mV hyperpolarizing pulse.

Ca^{2+} currents in a TEA^+-injected P cell are shown in Fig. 10A. The Ca^{2+} current had a peak value at potentials ranging from +10 to +20 mV (+18±5 mV in 18 cells). The Ca^{2+} current vanished at potentials ranging from +55 to +80 mV (with 8 mmol l^{-1} Ca^{2+} in the perfusing saline). These values presumably give an underestimate of the actual null-current potential of the Ca^{2+} current, since a residual outward current might still persist under our experimental conditions.

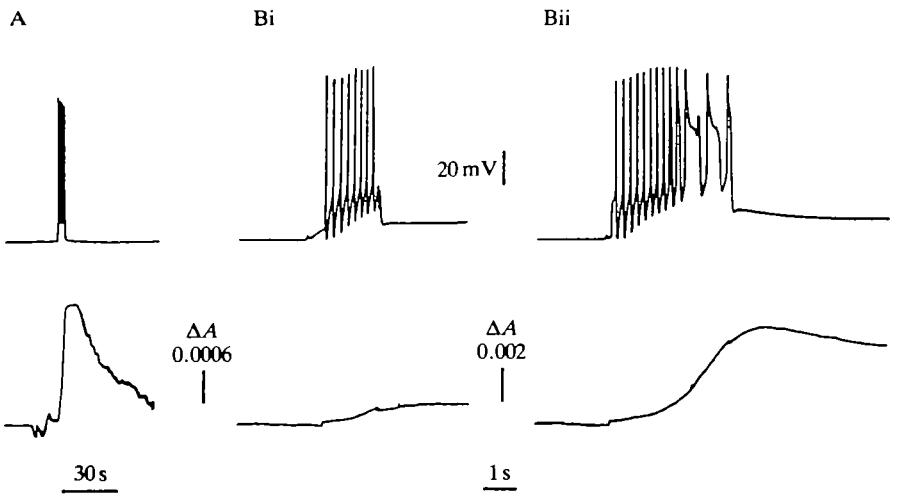

Fig. 9. Increase in intracellular $[Ca^{2+}]$ during firing and plateaus in the P1 cell. Changes in $[Ca^{2+}]_i$ (lower traces) were monitored by the differential absorbance change of Arsenazo III at two wavelengths (650 nm minus 690 nm). Intracellular dye injection was monitored by measuring the absorbance increase at 570 nm. The injection was stopped when the light intensity at 570 nm had decreased by half. (A) Transient increase in $[Ca^{2+}]_i$ induced by a brief spike burst in a P cell bathed in the standard Na^+-free saline. (Bi, Bii) From another P cell: a large $[Ca^{2+}]_i$ increase occurred during periods of prolonged spikes and plateaus. Vertical calibration in lower traces: relative change in absorbance (ΔA).

The peak Ca^{2+} current at +20 mV was 192±20 nA (N=17). Almost identical figures were observed in the large A cells (210±25 nA, N=15) and in the bursting cells (130–220 nA in five cells). The U cells had a smaller Ca^{2+} current (95±15 nA; N=6).

Ca^{2+} currents in P cells inactivated in long-lasting depolarizations. As already reported by several authors (see review by Eckert and Chad, 1984), inactivation was induced by both Ca^{2+} accumulation and depolarization. Ca^{2+}-induced inactivation was established from the effects of intracellular injections of EGTA into a TEA^+-injected cell bathed in the TEA^+ saline. Immediately upon cell impalement with the EGTA-filled microelectrode, the fast-inactivating phase was suppressed (Fig. 10B). An additional EGTA injection with negative current pulses induced a progressive increase in the Ca^{2+} current without any noticeable change in its time course. This increase might be attributable to the unblocking of Ca^{2+} channels and/or to the increase in the driving force acting on calcium ions, both resulting from the increase in the Ca^{2+}-buffering capacity of the cell.

The voltage-dependent inactivating process was investigated in P cells injected either with TEA^+ or with TEA^+ plus EGTA. A short (50–80 ms) test depolarizing pulse was applied after a 10 s conditioning depolarization. The Ca^{2+} current in the test pulse was progressively reduced by increasing the conditioning pulse ampli-

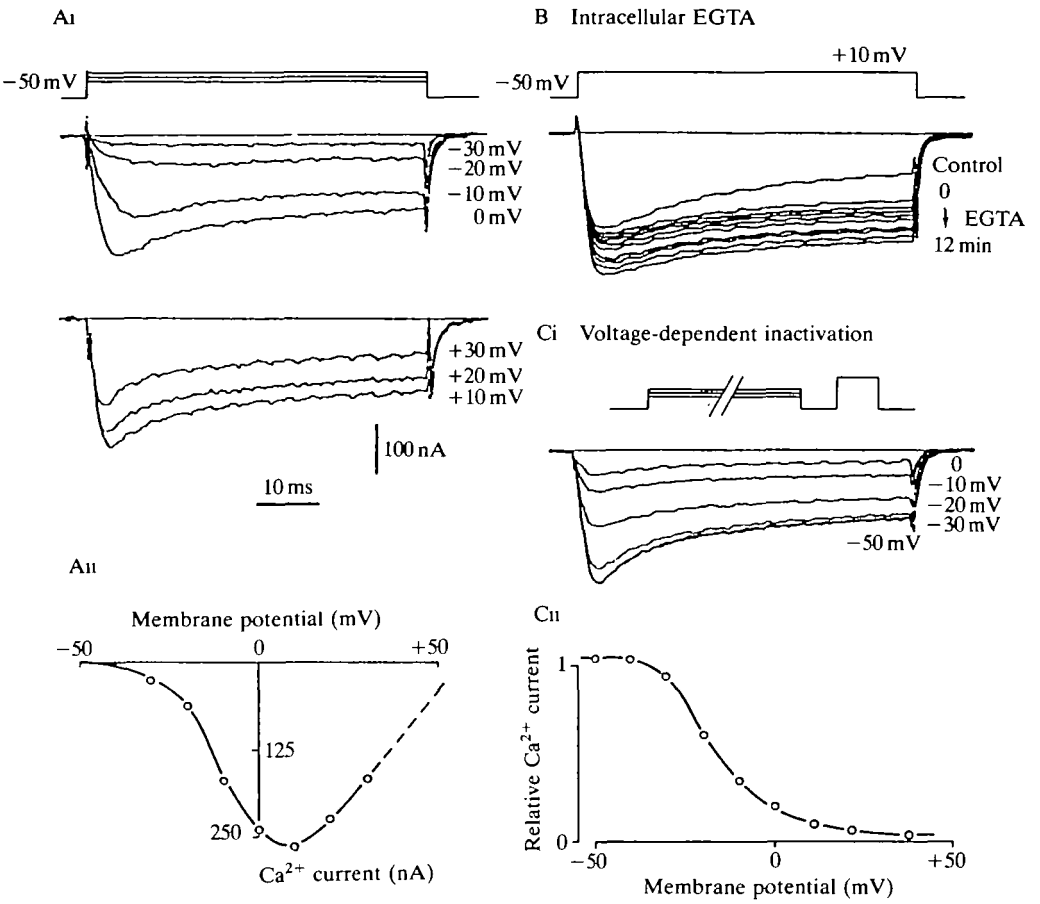

Fig. 10. Slowly inactivating calcium current in P cells. (A) P1 cell bathed in the Na^+-free saline containing 60 mmol l^{-1} TEA^+ and 10 mmol l^{-1} 4-AP. The cell was injected with TEA^+ to block K^+ currents. Currents were induced by step depolarizations at the levels indicated on current traces. Holding potential: −50 mV. (Aii) Peak Ca^{2+} current–voltage relationship. The extrapolated null-current potential was above +60 mV. (B) Effects of intracellular EGTA on the Ca^{2+} current. Holding potential: −50 mV; test pulse: +10 mV. Control: Ca^{2+} current recorded just before inserting the EGTA-filled microelectrode. The arrow marks the change in the Ca^{2+} current induced by a 12 min EGTA injection (with 100 nA negative current pulses). Injection of EGTA reduced the fast inactivating phase and increased the peak Ca^{2+} current. (C) Voltage-dependent inactivation of the Ca^{2+} current. Test pulse (+10 mV) applied after a 10 s conditioning pulse at the potential levels indicated in Ci. (Cii) Peak Ca^{2+} current (normalized to its control amplitude) *versus* conditioning potential.

tude (Fig. 10C). The peak Ca^{2+} current–conditioning potential curve was Z-shaped; inactivation was induced by potentials above −40 mV, and half-inactivation was observed at about −20 mV. Ca^{2+} current blockade was also induced by 10 s depolarizations to positive levels (from +20 to +80 mV). The shape and

location of the steady-state inactivating curve were not dependent on the presence of intracellular EGTA.

The residual Ca^{2+} current that persisted in prolonged depolarizations was therefore under voltage control, whereas the fast component of the inactivating process, which was suppressed by intracellular EGTA, was primarily produced by intracellular Ca^{2+} accumulation. Similar results were obtained in A and U cells. They are in line with data collected from various molluscan neurones (Eckert and Chad, 1984). The burst–plateau pattern observed in P cells does not, therefore, appear to have resulted from any unusual density or gating properties of Ca^{2+} channels.

Discussion

In most molluscan nerve cells, calcium ions make a consistent contribution to the depolarizing current that promotes spikes. In several instances, spikes persist in the absence of sodium in the bathing saline or after the addition of Na^+ channel blockers. These nerve cells generate Ca^{2+} spikes. Since Ca^{2+} channels are slowly and incompletely inactivated during prolonged depolarizations, sustained Ca^{2+} currents may result in uncontrolled depolarizations (see review by Eckert and Chad, 1984). Long-lasting spikes or even persistent depolarizations can be induced in these nerve cells by blocking the repolarizing K^+ currents. Several safeguards have been found to exist, however, against the occurrence of this uncontrolled regenerative Ca^{2+} entry, including the voltage-dependent and Ca^{2+}-dependent activation of repolarizing K^+ currents and the inactivation of Ca^{2+} channels. Consequently, Ca^{2+}-dependent spikes in molluscan neurones have a finite duration and are only moderately affected by repetitive pulsing.

The plateau-generating cells that we have identified in *Helix* ganglia display an unusual type of behaviour. Under repeated stimulation, they exhibit the progressive spike broadening that has been demonstrated previously in various molluscan neurones (Eckert and Lux, 1977; Aldrich *et al.* 1979; Gillette *et al.* 1980; Kits and Bos, 1982; Edstrom and Lukowiak, 1985). The broadening is particularly prominent, however, in P cells; the repolarizing phase is progressively delayed and slowed down and it finally aborts, leading to a prolonged plateau at a positive level. Similar long-lasting plateaus can be observed when neurones generating Ca^{2+}-dependent spikes are treated with K^+ channel blockers or when they are bathed in a saline in which calcium ions have been replaced by Ba^{2+}, which depresses repolarizing K^+ currents (Gola *et al.* 1977). The spike broadening in molluscan neurones has been attributed to frequency-dependent inactivation of voltage-sensitive K^+ currents (Aldrich *et al.* 1979) and/or to Ca^{2+}-induced inactivation of K^+ currents (Heyer and Lux, 1976). From these data, P cells seem to be characterized either by prominent inactivating processes acting on K^+ channels or by a relatively low density of K^+ channels. It will be shown in the following paper that the specificity of P cells involves both of these attributes.

The anatomy of P cells, as established by intracellular staining and nerve recordings, exhibits two structural features that are potentially relevant to their function: they send off axon branches into nerves which project to the entire foot muscle and to the mantle, and they receive information from the cerebral ganglia. These data suggest that P cells might be involved in motor functions related to motion. Despite an intensive search, however, we failed to detect any muscle movement when a P cell was fired. The anatomy of P cells is reminiscent of that of two giant *Aplysia* neurones, the R2 and LPl1 cells, located in the visceral and left pleural ganglia, respectively (Hughes and Tauc, 1963). Each cell sends axons to the right and left pedal ganglia from where they innervate the whole set of paropodial nerves. We have dye-filled several tens of neurones in the perioesophageal *Helix* ganglia. The axon distribution of the P cells appeared to be unique, since the main axon projections of the other neurones were to the four efferent nerves, with few if any secondary branches to the pedal ganglia. The same holds true with the R2 and LPl1 *Aplysia* neurones, which suggests that P cells may accomplish similar functions to those of the *Aplysia* neurones that control mucus secretion (Rayport *et al.* 1983). Additional experiments are required to clear up this point.

Under epi-illumination the P cell body had a white colour, which is generally produced by the presence of neurosecretory granules. These granules were observed at the electron microscopic level. The putative neurosecretory nature of P cells is in line with their electrophysiological behaviour. Spike broadening is particularly obvious in neurosecretory cells in general; caudo-dorsal cells in *Lymnaea stagnalis* can produce spikes lasting 125 ms during active secretory periods (Kits and Bos, 1982). A similar spike enlargement (5–16 times the initial spike duration) has been observed in the ventral white cells in the marine mollusc *Pleurobranchaea* (Gillette *et al.* 1980), in the neurosecretory bursting cells in *Helix* and *Aplysia* and in the terminals of the crab neurosecretory X-organ–sinus gland (Nagano and Cooke, 1987). In mammals, neuroendocrine cells, the electrical activity of which causes secretion of peptides, produce spike bursts (Andrew and Dudek, 1983) sustained by prolonged depolarized plateaus (Theodosis *et al.* 1983).

The spike broadening occurring in neurosecretory cells is commonly thought to facilitate synaptic transmission and the release of neurosecretory material. Our electrophysiological recordings on P cells were performed in the cell body and we had little information about the axon activity during periods of long-lasting depolarizations. When the cells were bathed in the normal Na^+-containing saline, fast voltage transients were superimposed on the plateau. Likewise, fast current transients were observed when the soma was depolarized under voltage-clamp conditions. These transients disappeared when P cells were bathed in Na^+-free saline; they were probably produced by remote Na^+-dependent axon spikes propagating distally.

The plateau, therefore, appears to have been restricted to the soma and the proximal axon; it has an appropriate shape and magnitude to serve as a driver potential supplying depolarizing current to an axonal impulse-initiating zone,

which might prolong the initial soma spike bursts and enhance the release of neurosecretory material.

References

ALDRICH, R. W., GETTING, P. A. AND THOMPSON, S. H. (1979). Mechanism of frequency dependent broadening of molluscan neurone soma spike. *J. Physiol., Lond.* **291**, 531–544.

ALTRUP, U. AND PETERS, M. (1982). Procedures of intracellular staining of neurons in the snail *Helix pomatia*. *J. Neurosci. Meth.* **5**, 161–165.

ANDREW, R. D. AND DUDEK, F. E. (1983). Burst discharge in mammalian neuroendocrine cells involves an intrinsic regenerative mechanism. *Science* **221**, 1050–1052.

CREST, M., EHILE, E., PIN, T., WATANABE, K. AND GOLA, M. (1990). Plateau-generating nerve cells in *Helix*: properties of the repolarizing voltage-gated and Ca^{2+}-activated potassium currents. *J. exp. Biol.* **152**, 211–241.

CROLL, R. P. (1986). Modified cobalt staining and silver intensification techniques for use with whole-mount gastropod ganglion preparations. *J. Neurobiol.* **17**, 569–576.

ECKERT, R. AND CHAD, J. E. (1984). Inactivation of Ca channels. *Prog. Biophys. molec. Biol.* **44**, 215–267.

ECKERT, R. AND LUX, H. D. (1977). Calcium-dependent depression of a late outward current in snail neurons. *Science* **197**, 472–475.

EDSTROM, J. P. AND LUKOWIAK, K. D. (1985). Frequency-dependent action potential prolongation in *Aplysia* pleural sensory neurones. *Neuroscience* **16**, 451–460.

GILLETTE, R., GILLETTE, M. U. AND DAVIS, W. J. (1980). Action potential broadening and endogenously sustained bursting are substrates of command ability in a feeding neuron of *Pleurobranchaea*. *J. Neurophysiol.* **43**, 669–685.

GOLA, M., CREST, M. AND HUSSY, N. (1986). Comparative study of calcium current contribution to paroxysmal depolarizations in invertebrate neurons. In *Epilepsy and Calcium* (ed. E.-J. Speckmann, H. Schulze and J. Walden), pp. 109–132. Munchen, Wien, Baltimore: Urban and Schwarzenberg.

GOLA, M., DUCREUX, C. AND CHAGNEUX, H. (1977). Ionic mechanisms of slow potential waves production in barium-treated *Aplysia* neurons. *J. Physiol., Paris* **73**, 407–440.

GORMAN, A. L. F. AND THOMAS, M. V. (1978). Changes in the intracellular concentration of free calcium ions in a pace-maker neurone, measured with the metallochromic dye Arsenazo III. *J. Physiol., Lond.* **275**, 357–376.

HEYER, C. B. AND LUX, H. D. (1976). Control of the delayed outward potassium currents in bursting pace-maker neurones of the snail *Helix pomatia*. *J. Physiol., Lond.* **262**, 349–382.

HUGHES, G. M. AND TAUC, L. (1963). An electrophysiological study of the anatomical relations of two giant nerve cells in *Aplysia depilans*. *J. exp. Biol.* **40**, 469–486.

JOHANSEN, J., YANG, J. AND KLEINHAUS, A. L. (1987). Voltage-clamp analysis of the ionic conductances in a leech neuron with a purely calcium-dependent action potential. *J. Neurophysiol.* **58**, 1468–1484.

KERKUT, G. A., FRENCH, M. C. AND WALKER, R. J. (1970). The location of axonal pathways of identifiable neurones of *Helix aspersa* using the dye Procion Yellow M-4R. *Comp. Biochem. Physiol.* **32**, 681–690.

KERKUT, G. A., LAMBERT, J. D. C., GAYTON, R. J., LOKER, J. E. AND WALKER, R. J. (1975). Mapping of nerve cells in the suboesophageal ganglia of *Helix aspersa*. *Comp. Biochem. Physiol.* **50A**, 1–25.

KITS, K. S. AND BOS, N. P. A. (1982). Na^+- and Ca^{++}-dependent components in action potentials of the ovulation hormone producing caudo-dorsal cells in *Lymnaea stagnalis* (Gastropoda). *J. Neurobiol.* **13**, 201–216.

LABOS, E. (1969). Repetition-sensitive soma response to de- and hyperpolarization of an identified *Helix* neuron. *Acta physiol. Acad. Hung.* **36**, 357–364.

LUX, H. D. AND HOFMEIER, G. (1982). Properties of a calcium- and voltage-activated potassium current in *Helix pomatia* neurons. *Pflügers Arch. ges. Physiol.* **394**, 61–69.

NAGANO, M. AND COOKE, I. M. (1987). Comparison of electrical responses of terminals, axons and somata of a peptidergic neurosecretory system. *J. Neurosci.* **7**, 634–648.

PIN, T. AND GOLA, M. (1984). Axonal mapping of neurosecretory *Helix* bursting cells. *Comp. Biochem. Physiol.* **78**A, 637–649.

RAYPORT, S. G., AMBRON, R. T. AND BARBIAZE, J. (1983). Identified cholinergic neurons R2 and LPl1 control mucus release in *Aplysia*. *J. Neurophysiol.* **49**, 864–876.

ROGAWSKI, M. A. (1985). The A-current: how ubiquitous a feature of excitable cells is it? *Trends Neurosci.* **8**, 214–219.

THEODOSIS, D. T., LEGENDRE, P., VINCENT, J. D. AND COOKE, I. (1983). Immunocytochemically identified vasopressin neurons in culture show slow, calcium-dependent electrical responses. *Science* **221**, 1052–1054.

WALKER, R. J., LAMBERT, J. D. C., WOODRUFF, G. N. AND KERKUT, G. A. (1970). Action potential shape and frequency as criteria for neuron identification in the snail *Helix aspersa*. *Comp. gen. Pharmac.* **1**, 409–425.